

# Generic Contrast Agents

Our portfolio is growing to serve you better. Now you have a *choice*.



[VIEW CATALOG](#)

# AJNR

## **Clinical Profiles and Patterns of Neurodegeneration in Amyotrophic Lateral Sclerosis: A Cluster-Based Approach Based on MR Imaging Metrics**

G. Milella, A. Introna, D.M. Mezzapesa, E. D'Errico, A. Fraddosio, M. Ucci, S. Zoccolella and I.L. Simone








This information is current as of May 17, 2025.

*AJNR Am J Neuroradiol* 2023, 44 (4) 403-409

doi: <https://doi.org/10.3174/ajnr.A7823>

<http://www.ajnr.org/content/44/4/403>

# Clinical Profiles and Patterns of Neurodegeneration in Amyotrophic Lateral Sclerosis: A Cluster-Based Approach Based on MR Imaging Metrics

 G. Milella,  A. Introna,  D.M. Mezzapesa,  E. D'Errico, A. Fraddosio,  M. Ucci,  S. Zoccolella, and  I.L. Simone

## ABSTRACT

**BACKGROUND AND PURPOSE:** The previous studies described phenotype-associated imaging findings in amyotrophic lateral sclerosis (ALS) with a prior categorization of patients based on clinical characteristics. We investigated the natural segregation of patients through a radiologic cluster-based approach without a priori patient categorization using 3 well-known prognostic MR imaging biomarkers in ALS, namely bilateral precentral and paracentral gyrus cortical thickness and medulla oblongata volume. We aimed to identify clinical/prognostic features that are cluster-associated.

**MATERIALS AND METHODS:** Bilateral precentral and paracentral gyri and medulla oblongata volume were calculated using FreeSurfer in 90 patients with amyotrophic lateral sclerosis and 25 healthy controls. A 2-step cluster analysis was performed using precentral and paracentral gyri (averaged pair-wise) and medulla oblongata volume.

**RESULTS:** We identified 3 radiologic clusters: 28 (31%) patients belonged to “cluster-1”; 51 (57%), to “cluster 2”; and 11 (12%), to “cluster 3.” Patients in cluster 1 showed statistically significant cortical thinning of the analyzed cortical areas and lower medulla oblongata volume compared with subjects in cluster 2 and cluster 3, respectively. Patients in cluster 3 exhibited significant cortical thinning of both paracentral and precentral gyri versus those in cluster 2, and this latter cluster showed lower medulla oblongata volume than cluster 3. Patients in cluster 1 were characterized by older age, higher female prevalence, greater disease severity, higher progression rate, and lower survival compared with patients in clusters 2 and 3.

**CONCLUSIONS:** Patients with amyotrophic lateral sclerosis spontaneously segregate according to age and sex-specific patterns of neurodegeneration. Some patients with amyotrophic lateral sclerosis showed an early higher impairment of cortical motor neurons with relative sparing of bulbar motor neurons (cluster 3), while others expressed an opposite pattern (cluster 2). Moreover, 31% of patients showed an early simultaneous impairment of cortical and bulbar motor neurons (cluster 1), and they were characterized by higher disease severity and lower survival.

**ABBREVIATIONS:** ALS = amyotrophic lateral sclerosis; ALSFRS-r = ALS Functional Rating Scale-Revised; CS = control subjects; IQR = interquartile range; MOv = medulla oblongata volume; ODI = onset-to-diagnosis interval; ParaCT = paracentral gyrus; PreCT = precentral gyrus

Amyotrophic lateral sclerosis (ALS) is a fatal neurodegenerative disease known for its extremely heterogeneous natural course.<sup>1</sup> Early identification of patients characterized by a faster disease progression rate is one of the primary goals in the field of motor neuron diseases to provide correct information about prognosis, care needs, and support services.

Several staging systems were previously proposed to stratify patients according to the phase of the disease and cognitive

profiles and to identify prognostic factors.<sup>2–7</sup> The feasibility of these staging systems has been proved in both trials and the clinical setting, by successfully allocating patients into specific disease categories. Several standard procedures have been proposed to guarantee interrater reliability in assessing the correct staging.<sup>8,9</sup> However, until now, clinical staging still requires the careful consideration of observed clinical parameters and relies invariably on the interpretation of reported symptoms and other potentially subjective factors. Therefore, several quantitative biomarkers,<sup>10,11</sup> beyond clinical parameters, have been proposed to correctly distinguish subgroups of patients according to different prognoses.

Among different “dry biomarkers,”<sup>12</sup> MR imaging has progressively acquired greater relevance to assess in vivo the extent of CNS damage in patients with ALS, given its accessibility and non-invasiveness. A recent review stated that the most disease-sensitive

Received September 20, 2022; accepted after revision February 20, 2023.

From the Neurology Unit (G.M., A.I., D.M.M., E.D., A.F., M.U., I.L.S.), Department of Basic Medical Sciences, Neurosciences and Sense Organs, University of Bari “Aldo Moro,” Bari, Italy; and Azienda Sanitaria Locale Bari (S.Z.), San Paolo Hospital, Bari, Italy.

Please address correspondence to Isabella Laura Simone, MD, Neurology Unit, Department of Basic Medical Sciences, Neurosciences and Sense Organs, University of Bari “Aldo Moro”; Piazza Giulio Cesare 11, 70124 Bari, Italy; e-mail: isabellalaura.simone@uniba.it

<http://dx.doi.org/10.3174/ajnr.A7823>

MR imaging patterns are located in motor regions.<sup>13</sup> Specifically, disease severity (expressed as ALS Functional Rating Scale-Revised [ALSFRS-r] score) and progression rate correlated with the mean cortical thickness of the motor area,<sup>14-18</sup> extramotor areas (eg, paracentral lobules),<sup>17,19</sup> and medulla oblongata volume (MOv).<sup>19-21</sup> These MR imaging metrics have also been proposed as predictive biomarkers of survival.<sup>20,22</sup>

Nonetheless, most imaging studies validated MR imaging metrics by describing phenotype-, genotype-, or stage-associated radiologic profiles<sup>23-25</sup> in a priori selected clinical categorizations (eg, spinal or bulbar onset, fast and slow progressors, prevalent upper or lower motor neuron impairment). An alternative interesting approach was recently performed by Bede et al,<sup>26</sup> which used cluster analysis of pooled imaging data and subsequent analysis of cluster-associated clinical characteristics. Using a large unsegregated MR imaging data set and 74 MR imaging metrics, the authors found that patients with ALS spontaneously segregated in 2 clusters mainly according to 3 specific areas, namely superior lateral temporal and superior and inferior frontal gyri. The 2 clusters exhibited different frontotemporal impairment on MR imaging and the prevalence of *C9orf72* mutation carriers. In line with this study, Tan et al<sup>27</sup> found that patients with ALS could be divided into 3 subgroups (pure motor neuron; orbitofrontal and temporal involvement; posterior cingulate cortex, parietal white matter temporal operculum and cerebellum) using a connectome-based clustering algorithm among 68 cortical regions, 15 subcortical structures, and all the white matter tracts between these latter regions.

Different from these latter studies, we restricted our cluster-based analysis to MR imaging metrics identified as core features of disease severity and survival in ALS by previous reports, namely cortical thickness of the precentral gyrus (PreCT)<sup>22</sup> and paracentral gyrus (ParaCT)<sup>22</sup> and MOv.<sup>20</sup> Thus, we aimed to identify the clinical and prognostic features of the different radiologic clusters.

## MATERIALS AND METHODS

### Ethics Approval

We confirm that we have read AJNR's position on issues involved in ethical publication and affirm that this report is consistent with those guidelines. Ethics approval was waived by the local ethics committee, considering that all the procedures being performed were part of the routine care (study No. 6778).

### Population

A total of 90 incident patients with ALS referred to our ALS tertiary center between 2018 and 2020 were consecutively recruited at the time of diagnosis. A careful diagnostic work-up was performed to exclude ALS-mimicking diseases. All patients met the criteria for clinically definite, probable, or possible ALS according to the El Escorial-revised criteria.<sup>4</sup> Exclusion criteria included prior cerebrovascular events, traumatic brain injury, neurosurgical procedures, as well as neoplastic, paraneoplastic, or neuroinflammatory comorbidities.

None of the patients fulfilled the criteria for ALS and frontotemporal dementia according to the Strong criteria.<sup>5</sup>

Demographic characteristics and clinical data have been registered and collected by experienced neurologists of the ALS team. We recorded the following demographic and clinical variables: age at symptom onset, sex, onset-to-diagnosis interval (ODI), age at diagnosis (corresponding to the first neurologic clinical evaluation), site of symptom onset, and clinical phenotype.<sup>1</sup>

All patients were functionally evaluated using the ALSFRS-r.<sup>28</sup> The progression rate was calculated using the following formula:  $(48 - \text{ALSFRS-r}) / \text{disease durations (months)}$ .<sup>29</sup>

Longitudinal clinical evaluations were performed at 4- to 6-month intervals, and data regarding death or tracheostomy were recorded. The censoring date was set at March 31, 2022. Tracheostomy or death (if it occurred) were considered as a composite outcome.

Control subjects (CS) consisted of 25 subjects, not affected by inflammatory, autoimmune, and vascular or neurodegenerative diseases, without a family history of ALS and without abnormal findings on brain MR imaging.

### MR Imaging Acquisitions

All participants underwent MR imaging on a 1.5T MR imaging scanner (Philips) at Azienda Ospedaliero Universitaria Policlinico of Bari. Specifically, patients with ALS underwent MR imaging at the time of diagnosis, concurrent with their first neurologic evaluation. Routine T1-, T2-weighted, and FLAIR sequences were performed to exclude other causes of focal or diffuse brain damage, including lacunar and extensive cerebrovascular lesions. 3D structural MR imaging was acquired using a T1-weighted MPRAGE sequence (TR/TE/flip angle = 25.00 ms/4.60 ms/30.00°, FOV = 240 mm, matrix = 256 × 256, voxel size = 0.93 × 0.93 × 1.0 mm<sup>3</sup>).

### Cortical Thickness Analysis and Volumetric Analysis

FreeSurfer software, Version 7.1 (<http://surfer.nmr.mgh.harvard.edu>) was used to assess cortical thickness. Processing steps included correction for magnetic field inhomogeneity, alignment to a specific atlas,<sup>30</sup> skull removal, and segmentation of voxels into GM, WM, and CSF. Cortical thickness was then calculated on the basis of the shortest distance of 2 surfaces: the interface between GM and WM and the pial surface. The anatomic labels of the Desikan-Killiany atlas<sup>31</sup> were used to calculate average cortical thickness in the precentral and paracentral cortical regions in the left and right cerebral hemispheres separately.

MOv was obtained using the FreeSurfer tool “segmentBS.sh.”<sup>32</sup> Segmentation (<https://surfer.nmr.mgh.harvard.edu/fswiki/BrainstemSubstructures>) was conducted using a robust and accurate Bayesian algorithm, relying on a probabilistic atlas of the brainstem and neighboring anatomic structures implemented in FreeSurfer.<sup>32</sup> Additionally, from each preprocessed T1-weighted data set, total intracranial volume was calculated using FreeSurfer. Raw volumetric values of the medulla oblongata were corrected for the total intracranial volume using the residual method.<sup>33</sup>

**Statistical Analysis.** The bilateral PreCT and ParaCT were averaged pair-wise and, together with MOv, were included in the 2-step cluster analysis. The choice of using the left and right precentral and paracentral cortical thicknesses averaged pair-wise is

consistent with previous studies that showed that cortical atrophy in these latter regions occurred early and bilaterally, especially in patients with ALS with bulbar-onset<sup>34</sup> and, irrespective of the side of first limb weakness, in patients with ALS with spinal onset.<sup>35</sup> Furthermore, because interhemispheric asymmetry was found in healthy subjects,<sup>36</sup> the inclusion of MR imaging metrics belonging to both the right and left hemispheres could have biased the entire analysis by finding clusters that are subject-related and not disease-related. Therefore, we included the pair-wise average precentral and paracentral cortical thickness, to provide an overall measure of cortical atrophy, as performed elsewhere.<sup>22,26</sup>

Both cortical thickness and volumetric measures were minimum-maximum normalized to a 0–1 scale, to account for different measurements scales. The 2-step cluster analysis was performed using the Euclidean distance measure. The number of clusters was not fixed a priori, and the Bayesian information criterion was used to determine the number of clusters. On the basis of cluster membership of individual patients, cluster sizes were determined and silhouette analyses were run using the STATS CLUS SIL extension of SPSS (IBM).<sup>26</sup>

ANCOVA was performed to evaluate differences in MR imaging metrics between the following groups: first, between CS and each radiologic ALS cluster and then among patients with ALS belonging to different clusters. In the analysis, PreCT and ParaCT and MOv were included as dependent variables, and study groups as categoric independent variables. Age at the first neurologic evaluation (time of diagnosis) and sex were considered potential confounding factors,<sup>37</sup> and they were used as covariates.

Demographic and clinical variables of the entire ALS population and of each cluster patient were reported as median (along with interquartile range [IQR]) or frequencies (percentages) for continuous and categoric variables, respectively. Group differences in the demographic and clinical variables were evaluated using a Mann-Whitney *U* test for continuous variables and the  $\chi^2$  or Fisher exact test for categoric variables.

To evaluate the different prognoses of each cluster, we dichotomized all patients with ALS into long and short survivors using the 2-step cluster analysis.<sup>38</sup> Categoric variables (reaching or not reaching the end point) and continuous variables (time elapsed between symptoms onset and censoring date or end points) were included in the model. Logistic regression was used to test the different percentages of short and long survivors in each cluster. The results were reported as OR and 95% CI. Last, Kaplan-Meier survival curves were used to illustrate the distribution of survival, and log-rank tests were used to test for differences among different radiologic clusters.

## RESULTS

### Clinical and Demographic Characteristics of the ALS Population and CS

The median age at symptom onset was 57 years, and the median ODI was 10 months. The spinal onset of disease was more frequent than bulbar onset (74% and 26%, respectively). Sixty-eight patients (76%) were classified as classic ALS phenotypes.<sup>1</sup> Twenty-two (24%) patients were classified as having “definite ALS” according to the El Escorial-revised criteria.<sup>4</sup> Sixty-five (72%) patients reached the composite outcome (tracheostomy or death)

at the censoring date. The estimated median survival time from symptom onset to combined outcome was 47 months (Table).

CS were sex- and age-matched to patients with ALS with a median age of 54 years (IQR = 45–57 years) and a male-to-female ratio of 14:11 (56% male and 44% female).

### MR Imaging Metrics

Two-step cluster analysis identified 3 distinct clusters of anatomic disease burden distribution: among all patients with ALS, 28 (31%) belonged to cluster 1; 51 (57%), to cluster 2; and 11, (12%) to cluster 3. The silhouette coefficient of 0.6 indicates reasonable cohesion and separation according to Kaufman and Rousseeuw.<sup>39</sup>

In comparison with CS, patients with ALS in cluster 1 exhibited significantly lower values of both PreCT and ParaCT and MOv ( $P < .001$  for all). Patients with ALS in cluster 2 had lower values of MOv compared with CS ( $P < .001$ ), whereas patients with ALS in cluster 3 showed significantly lower PreCT and ParaCT values ( $P = .001$ ), but no differences in MOv (Fig 1).

Patients with ALS in cluster 1 showed significantly lower PreCT and ParaCT values compared with those in cluster 2 ( $P < .001$  for both), but not patients in cluster 3. Furthermore, the patients with ALS in cluster 1 had lower MOv values than those in cluster 3 ( $P < .001$ ), but not patients in cluster 2. On the other hand, patients with ALS in cluster 2 exhibited significantly lower values of MOv ( $P < .001$ ) compared with those in cluster 3, and in turn, this latter cluster had lower values of both PreCT and ParaCT than cluster 2 ( $P = .001$  for both) (Fig 1).

### Clinical and Demographic Features of the 3 Clusters

The Table shows the cluster-associated ALS clinical and demographic features.

The 3 clusters differed in age and sex: specifically, patients with ALS in cluster 1 were older than those in cluster 2 and cluster 3 ( $P = .045$  and  $P = .001$ , respectively), while no differences were found between these latter 2 groups (Table). Male prevalence was 57% and 82% in clusters 2 and 3, respectively, while female prevalence was 68% in cluster 1 ( $P = .035$  and  $P = .005$ , respectively).

No statistically significant differences were found in the ODI among the 3 groups. A spinal onset of the disease was found in all patients with ALS in cluster 3 and in about 70% of patients with ALS in both clusters 1 and 2. Patients with ALS in cluster 1 also had a higher diagnostic certainty, expressed by a higher percentage of “definite ALS” according to the El Escorial-revised criteria, compared with those in cluster 2 (43% versus 16%,  $P < .001$ ) and cluster 3 (43% versus 18%,  $P = .017$ ).

Patients with ALS in cluster 1 had an overall higher disease severity, expressed by lower ALSFRS-r scores than patients in both cluster 2 and cluster 3 ( $P = .001$  and  $P < .001$ , respectively), while no differences were found between these latter 2 groups. Furthermore, patients with ALS in cluster 1 showed a higher progression rate compared with those in cluster 2 and cluster 3 ( $P = .002$  and  $P = .02$ , respectively).

### Survival Analysis

Among our study cohort, 26 patients were included in the long survivors' group with a median time of observation of 57 months (IQR = 45–80 months), and none of them reached the composite

**Association between MR imaging clusters and clinical features in patients with ALS<sup>a</sup>**

	ALS Population (n = 90)	Cluster 1 (n = 28)	Cluster 2 (n = 51)	Cluster 3 (n = 11)	P Value
Age at onset (median) (IQR) (yr)	57 (50–65)	67 (62–70)	41 (44–54)	46 (45–54)	$P = .045^b$ $P = .001^c$ $P = ns^d$
Sex (No. of patients) (male/female)	47:43	9:19	29:22	9:2	$P = .035^b$ $P = .005^c$ $P = ns^d$
Site of onset (spinal/bulbar) (No. of patients)	67/23	20/8	36/15	11/0	$P = ns^b$ $P = .047^c$ $P = .039^d$
ALS phenotypes: classic/bulbar/flail arm/flail leg/pyramidal/respiratory/ PLMN/PUMN (No. of patients)	68/7/0/0/0/0/ 15/0	25/2/0/0/0/0/ 0/1/0	34/5//0/0/0/0/ 0/12/0	9/0//0/0/0/0/ 0/2/0	$P = ns^b$ $P = ns^c$ $P = ns^d$
El Escorial-revised, categories: definite/ probable/possible (No. of patients)	22/36/32	12/14/2	8/18/25	2/4/5	$P < .001^b$ $P = .017^c$ $P = ns^d$
ODI (median) (IQR) (mo)	10.07 (6.08–19.27)	9.18 (6.08–14.32)	11.73 (6.23–19.53)	8.97 (4.07–19.27)	$P = ns^b$ $P = ns^c$ $P = ns^d$
ALSFRS-r (median score) (IQR)	38 (34–42)	34 (31–37)	40 (35–43)	40 (38–43)	$P = .001^b$ $P < .001^c$ $P = ns^d$
Progression rate (median) (IQR)	0.83 (0.45–1.38)	1.26 (0.68–2.84)	0.70 (0.29–1.20)	0.80 (0.45–1.12)	$P = .002^b$ $P = .022^c$ $P = ns^d$
Long/short survivors (No. of patients)	26/64	3/25	17/34	6/5	$P = .032^b$ $P = .008^c$ $P = ns^d$
Survival time from symptom onset to composite outcome (median) (estimated median) (95% CI) (mo)	46.63 (37.95–55.31)	34.5 (22.39–46.6)	46.63 (35.4–57.87)	72.73 (42.98–102.47)	$P = .043^b$ $P = .004^c$ $P = ns^d$

**Note:**—ns indicates not significant; PLMN, prevalent lower motor neuron; PUMN, prevalent upper motor neuron.

<sup>a</sup>Group differences in the demographic and clinical variables were evaluated using a Mann-Whitney *U* test for continuous variables and  $\chi^2$  tests for discrete variables. Log-rank tests were used to test for differences in survival between different radiologic clusters.

<sup>b</sup>Cluster 1 versus cluster 2.

<sup>c</sup>Cluster 1 versus cluster 3.

<sup>d</sup>Cluster 2 versus cluster 3.

outcome at the censoring date (Table). The short survivors' group was characterized by 64 patients with a median time of observation of 36 months (IQR = 24–52 months), and all of them reached the composite outcome. Patients in cluster 1 showed a 4- and 10-fold risk of belonging to the short survivors' group compared with those in clusters 2 and 3, respectively ( $P = .036$  with hazard risk: 4.17 and a 95% CI, 1.11–15.87 and  $P = .007$  with hazard risk: 10 and a 95% CI, 1.85–52.63, respectively).

Kaplan-Meier survival curves revealed that patients with ALS in cluster 1 showed a worse prognosis compared with patients in cluster 2 (log-rank: 4.10,  $P = .043$ ) and cluster 3 (log-rank: 8.22,  $P = .004$ ). No significant differences in overall survival from the onset of symptoms were detected between patients in these latter 2 groups (Table and Fig 2).

## DISCUSSION

In the present study, we performed a data-driven analysis to identify the radiologic clustering of newly diagnosed patients with ALS, in relation to 3 well-known neuroanatomic loci involved in ALS disease, namely the PreCT<sup>22</sup> and ParaCT<sup>22</sup> and the medulla oblongata.<sup>20</sup> Our data suggested that already at the time of diagnosis, patients with ALS showed specific patterns of neurodegeneration, with a prevalent impairment of the motor

and extramotor cortex, cluster 3; MOv, cluster 2; or all 3 MR imaging measures, cluster 1. This latter group of patients was characterized by older age, higher female prevalence, greater disease severity expressed by lower ALSFRS-r scores, a higher progression rate, and lower median survival.

MR imaging data-driven approaches potentially have several advantages in clinical practice because they do not require a previous integration of clinical data. Unlike in interesting previous studies that first applied this approach,<sup>26,27</sup> we focused our cluster-based analysis on CNS-selected areas that are already found to be associated with survival<sup>20,22</sup> and disease severity.<sup>17,21,40</sup> Restricting the cluster-based analysis to the motor cortical areas and medulla oblongata, we first found that a considerable proportion (57%) of patients with ALS (belonging to cluster 2) showed greater involvement of the medulla already at the time of diagnosis. Second, a small subgroup of the ALS cohort (cluster 3, 12%) had early involvement of the motor and extramotor cortices with relative preservation of the medulla oblongata. Finally, 31% of those with ALS (cluster 1) showed wider and more prominent involvement of both cortical regions and medulla oblongata volume. These results appear in line with previous neuropathologic and neuroradiologic studies. Indeed, the earlier brainstem involvement found in 88% of our patients (clusters 1 and 2)

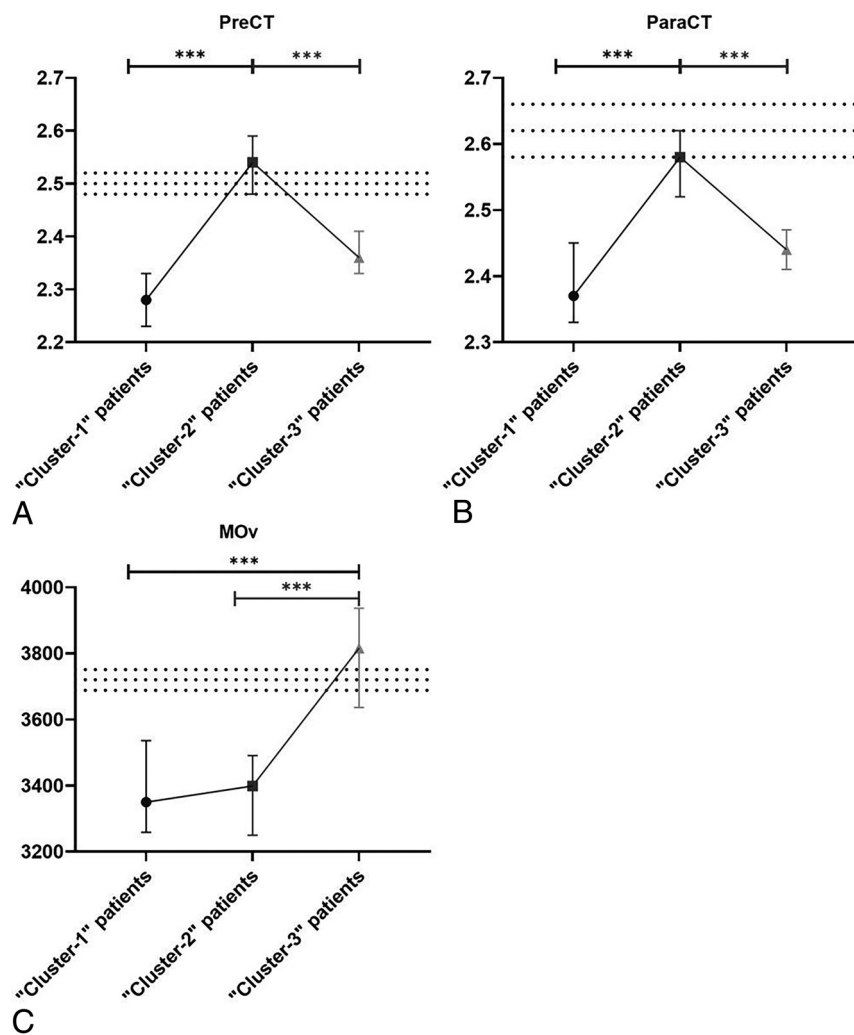


**FIG 1.** Estimated marginal means with SDs of the PreCT (A), ParaCT (B), and MOv (C) are plotted for each radiologic cluster adjusted for age and sex. Estimated marginal means and SDs of the CS are reported in the black dotted lines. The asterisk indicates  $P < .001$ .

agrees with the findings of Brettschneider et al,<sup>41</sup> who reported that brainstem involvement represents “stage 1” in ALS pathology. Nonetheless, the early involvement of cortical motor neurons with subsequent spread along contiguous neuroanatomic regions in fewer patients (43% belonging to clusters 1 and 3) may support the role of these brain regions in the onset of ALS disease, as recently postulated by a radiologic study of Schito et al.<sup>42</sup>

Finally, to explain the simultaneous and early involvement of both cortical regions and the medulla oblongata volume in patients with ALS in cluster 1, we referred to the most accredited model of ALS disease propagation reported in the literature.<sup>43</sup> Indeed, also in these latter patients, the onset of the disease could have been focal in the cortical and/or the brainstem motor neurons, as postulated by Ravits,<sup>43</sup> but a rapid spread of the disease along the neuroaxis would not allow us to detect the first neuroanatomic region involved, even at the onset of the disease in these patients. Alternatively, the onset of disease could have been due to “multi-focal hits” with simultaneous involvement of cortical and brainstem motor neurons as recently postulated and demonstrated through an elegant neurophysiologic study by Sekiguchi et al.<sup>44</sup>

In addition, we observed that patients with ALS with wider impairment of both cortical and medulla oblongata regions (cluster 1) were characterized by an older age at onset and higher female prevalence. The effect of both age at onset and sex on MR imaging metrics was previously and extensively reported.<sup>37,45–47</sup> On the basis of previous literature data, older age at symptom onset might provide a vulnerable substrate for faster and more severe disease propagation,<sup>45</sup> while ALS sex-related brain functional and structural changes have been reported with controversial results.<sup>37,48</sup>

According to a very recent study, there is increasing evidence that ALS disease follows different patterns of neurodegeneration that are age- and sex-specific. Tan et al<sup>27</sup> found a cluster of patients with ALS characterized by predominant involvement of the PreCT, younger age, and higher male prevalence. In addition, the authors described another cluster characterized by female prevalence and older age with wide posterior cingulate, parietal, cerebellar motor, temporal, and corpus medullare neurodegeneration.<sup>27</sup> Overall, all these findings agreed with a previous population-based study that reported the interaction between age and female sex, with women more affected than men at older ages.<sup>49</sup>

The most intriguing findings of our study were the clinical consequences of the radiologic clustering of patients

with ALS. Indeed, patients with ALS in cluster 1 with a wider impairment of both cortical and medulla oblongata regions were characterized by overall higher disease severity (expressed as lower scores of the total ALSFRS-r score), higher progression rate, and worse outcome, compared with patients in clusters 2 and 3. As stated above, several previous studies have underlined how PreCT, ParaCT and MOv could be used singularly as indicators of ALS disease aggressiveness.<sup>14,17,20,21,40</sup> Nevertheless, these latter approaches relied invariably on the interpretation of clinical data that could somehow be misleading. An example of this limitation was recently aroused by Ferrea et al,<sup>25</sup> who demonstrated through a discriminant analysis that patients with ALS with prevalent upper and lower motor neuron impairment could be differentiated by specific MR imaging metrics of the motor and extramotor regions. However, the same authors reported that the clinical distinction between ALS phenotypes (prevalent upper and prevalent lower motor neurons and classic ALS) is somewhat heterogeneous; therefore, they included this concept as a limit of their study.<sup>25</sup> Instead, using a cluster-based approach without a priori clinical categorization of patients with ALS, we overcame the

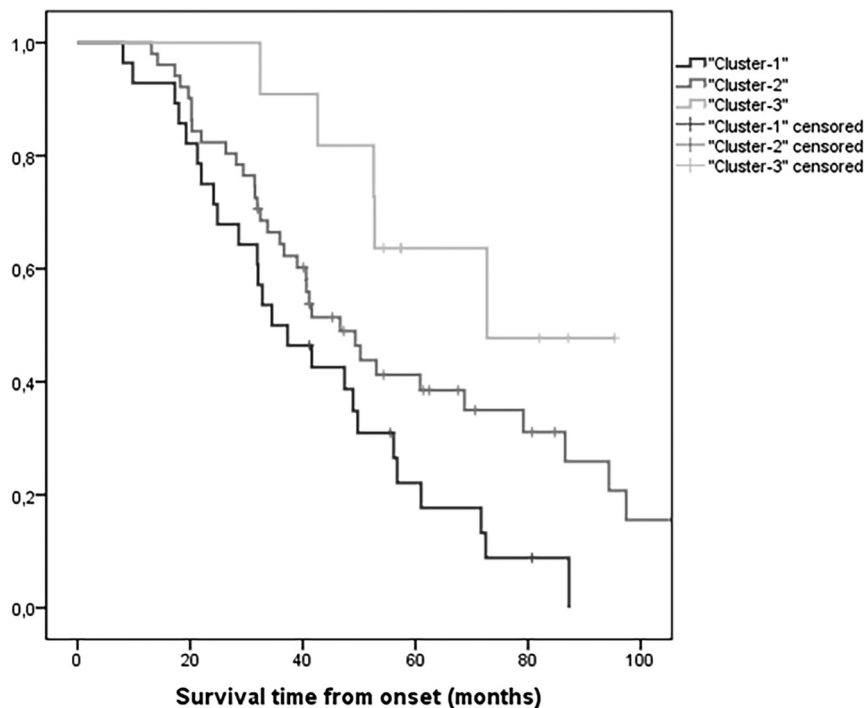


**FIG 2.** Kaplan Mayer survival curves in patients with ALS stratified according to radiologic clusters.

intrinsic limitation of investigating the correlation between clinical characteristics and each neuroanatomic structure, and we demonstrated that both the impairment of cortical and medullar regions corresponded simultaneously with the severity, rate of progression, and survival in ALS disease. Furthermore, a data-driven analysis could also overcome the potentially subjective interpretation of reported symptoms, which could be biased by “recall error,” especially in patients with a long-lasting disease.

The main limitation of our study is the lack of a longitudinal MR imaging analysis, which, instead, would have better defined the trajectories of the disease burden and the rate of decline of MR imaging metrics according to different clusters. Another limitation is the lack of neuropsychological assessment, which would guarantee a better characterization of cognitive profiles among radiologic clusters. Last, in our study, we included only patients with a definite, probable, or possible diagnosis of ALS. The inclusion of patients with ALS with pure lower motor neuron impairment, as well as progressive muscular atrophy or progressive lateral sclerosis, may be of potential interest to evaluate whether these subtypes segregate from ALS on the basis of their radiologic profiles.<sup>50,51</sup>

## CONCLUSIONS

We demonstrated that radiologic clustering of newly diagnosed patients with ALS could have clinical and prognostic implications and could unravel some aspects of the extreme phenotypic heterogeneity of ALS disease. Patients with undoubtedly more advanced and extended disease burdens (cluster 1) should be carefully evaluated to propose therapeutic interventions, such as timely positioning of percutaneous endoscopic gastrostomy or tracheostomy.

## ACKNOWLEDGMENT

We are grateful to the patients with ALS and their families.

Disclosure forms provided by the authors are available with the full text and PDF of this article at [www.ajnr.org](http://www.ajnr.org).

## REFERENCES

- Chio A, Calvo A, Moglia C, et al. **Phenotypic heterogeneity of amyotrophic lateral sclerosis: a population based study.** *J Neurol Neurosurg Psychiatry* 2011; 82:740–46 [CrossRef Medline](#)
- Fang T, Al Khleifat A, Stahl DR, et al. **Comparison of the King's and MiToS staging systems for ALS.** *Amyotroph Lateral Scler Frontotemporal Degener* 2017;18:227–32 [CrossRef Medline](#)
- Tramacere I, Dalla Bella E, Chio A, et al. **The MITOS system predicts long-term survival in amyotrophic lateral sclerosis.** *J Neurol Neurosurg Psychiatry* 2015;86:1180–85 [CrossRef Medline](#)
- Brooks BR, Miller RG, Swash M, et al; World Federation of Neurology Research Group on Motor Neuron Diseases. **El Escorial revisited: revised criteria for the diagnosis of amyotrophic lateral sclerosis.** *Amyotroph Lateral Scler Motor Neuron Disord* 2000;1:293–99 [CrossRef Medline](#)
- Strong MJ, Abrahams S, Goldstein LH, et al. **Amyotrophic lateral sclerosis: frontotemporal spectrum disorder (ALS-FTSD)—revised diagnostic criteria.** *Amyotroph Lateral Scler Frontoporal Degener* 2017;18:153–74 [CrossRef Medline](#)
- Balendra R, Jones A, Jivraj N, et al; UK-MND LiCALS Study Group, Mito Target ALS Study Group. **Use of clinical staging in amyotrophic lateral sclerosis for phase 3 clinical trials.** *J Neurol Neurosurg Psychiatry* 2015;86:45–49 [CrossRef Medline](#)
- Introna A, Milella G, Morea A, et al. **King's College progression rate at first clinical evaluation: a new measure of disease progression in amyotrophic lateral sclerosis.** *J Neurol Sci* 2021;431:120041 [CrossRef Medline](#)
- Balendra R, Al Khleifat A, Fang T, et al. **A standard operating procedure for King's ALS clinical staging.** *Amyotroph Lateral Scler Frontoporal* 2019;20:159–64 [CrossRef Medline](#)
- Bakers JN, de Jongh AD, Bunte TM, et al. **Using the ALSFRS-R in multicentre clinical trials for amyotrophic lateral sclerosis: potential limitations in current standard operating procedures.** *Amyotroph Lateral Scler Frontoporal* 2021;23:500–07 [CrossRef Medline](#)
- Gaiani A, Martinelli I, Bello L, et al. **Diagnostic and prognostic biomarkers in amyotrophic lateral sclerosis: neurofilament light chain levels in definite subtypes of disease.** *JAMA Neurol* 2017;74:525–32 [CrossRef Medline](#)
- Scarafino A, D'Errico E, Introna A, et al. **Diagnostic and prognostic power of CSF Tau in amyotrophic lateral sclerosis.** *J Neurol* 2018;265:2353–62 [CrossRef Medline](#)
- Verber NS, Shephard SR, Sassani M, et al. **Biomarkers in motor neuron disease: a state of the art review.** *Front Neurol* 2019;10:291 [CrossRef Medline](#)
- Grolez G, Moreau C, Danel-Brunaud V, et al. **The value of magnetic resonance imaging as a biomarker for amyotrophic lateral sclerosis: a systematic review.** *BMC Neurol* 2016;16:155 [CrossRef Medline](#)
- Agosta F, Valsasina P, Riva N, et al. **The cortical signature of amyotrophic lateral sclerosis.** *PLoS One* 2012;7:e42816 [CrossRef Medline](#)

15. Schuster C, Kasper E, Machts J, et al. **Focal thinning of the motor cortex mirrors clinical features of amyotrophic lateral sclerosis and their phenotypes: a neuroimaging study.** *J Neurol* 2013;260:2856–64 [CrossRef Medline](#)
16. Walhout R, Westeneng H-J, Verstraete E, et al. **Cortical thickness in ALS: towards a marker for upper motor neuron involvement.** *J Neurol Neurosurg Psychiatry* 2015;86:288–94 [CrossRef Medline](#)
17. Mezzapesa DM, D'Errico E, Tortelli R, et al. **Cortical thinning and clinical heterogeneity in amyotrophic lateral sclerosis.** *PLoS One* 2013;8:e80748 [CrossRef Medline](#)
18. Distaso E, Milella G, Mezzapesa DM, et al. **Magnetic resonance metrics to evaluate the effect of therapy in amyotrophic lateral sclerosis: the experience with edaravone.** *J Neurol* 2021;268:3307–15 [CrossRef Medline](#)
19. Senda J, Kato S, Kaga T, et al. **Progressive and widespread brain damage in ALS: MRI voxel-based morphometry and diffusion tensor imaging study.** *Amyotroph Lateral Scler* 2011;12:59–69 [CrossRef Medline](#)
20. Milella G, Introna A, Ghirelli A, et al. **Medulla oblongata volume as a promising predictor of survival in amyotrophic lateral sclerosis.** *Neuroimage Clin* 2022;34:103015 [CrossRef Medline](#)
21. Li H, Zhang Q, Duan Q, et al. **Brainstem involvement in amyotrophic lateral sclerosis: a combined structural and diffusion tensor MRI analysis.** *Front. Neurosci* 2021;15:675444 [CrossRef Medline](#)
22. Schuster C, Hardiman O, Bede P. **Survival prediction in amyotrophic lateral sclerosis based on MRI measures and clinical characteristics.** *BMC Neurol* 2017;17:73 [CrossRef Medline](#)
23. Finegan E, Li Hi Shing S, Chipika RH, et al. **Widespread subcortical grey matter degeneration in primary lateral sclerosis: a multimodal imaging study with genetic profiling.** *Neuroimage Clin* 2019;24:102089 [CrossRef Medline](#)
24. Consonni M, Dalla Bella E, Contarino VE, et al. **Cortical thinning trajectories across disease stages and cognitive impairment in amyotrophic lateral sclerosis.** *Cortex* 2020;131:284–94 [CrossRef Medline](#)
25. Ferrea S, Junker F, Korth M, et al. **Cortical thinning of motor and non-motor brain regions enables diagnosis of amyotrophic lateral sclerosis and supports distinction between upper- and lower-motor neuron phenotypes.** *Biomedicines* 2021;9:1195 [CrossRef Medline](#)
26. Bede P, Murad A, Lope J, et al. **Clusters of anatomical disease-burden patterns in ALS: a data-driven approach confirms radiological subtypes.** *J Neurol* 2022;268:4404–13 [CrossRef Medline](#)
27. Tan HH, Westeneng HJ, Nitert AD, et al. **MRI clustering reveals three ALS subtypes with unique neurodegeneration patterns.** *Ann Neurol* 2022;92:1030–45 [CrossRef Medline](#)
28. Cedarbaum JM, Stambler N, Malta E, et al. **The ALSFRS-R: a revised ALS functional rating scale that incorporates assessments of respiratory function—BDNF ALS Study Group (Phase III).** *J Neurol Sci* 1999;169:13–21 [CrossRef Medline](#)
29. Kimura F, Fujimura C, Ishida S, et al. **Progression rate of ALSFRS-R at time of diagnosis predicts survival time in ALS.** *Neurology* 2006;66:265–67 [CrossRef Medline](#)
30. Grachev ID, Berdichevsky D, Rauch SL, et al. **A method for assessing the accuracy of intersubject registration of the human brain using anatomic landmarks.** *Neuroimage* 1999;9:250–68 [CrossRef Medline](#)
31. Hutton C, Draganski B, Ashburner J, et al. **A comparison between voxel-based cortical thickness and voxel-based morphometry in normal aging.** *Neuroimage* 2009;48:371–80 [CrossRef Medline](#)
32. Iglesias JE, Van Leemput K, Bhatt P, et al; Alzheimer's Disease Neuroimaging Initiative. **Bayesian segmentation of brainstem structures in MRI.** *NeuroImage* 2015;113:184–95 [CrossRef Medline](#)
33. Pintzka C, Hansen TI, Evensmoen H, et al. **Marked effects of intracranial volume correction methods on sex differences in neuroanatomical structures: a HUNT MRI study.** *Front Neurosci* 2015;9:238 [CrossRef Medline](#)
34. Steinbach R, Prell T, Gaur N, et al. **Patterns of grey and white matter changes differ between bulbar and limb onset amyotrophic lateral sclerosis.** *Neuroimage Clin* 2021;30:102674 [CrossRef Medline](#)
35. Zhang Q, Mao C, Jin J, et al. **Side of limb-onset predicts laterality of gray matter loss in amyotrophic lateral sclerosis.** *BioMed Res Int* 2014;2014:e473250 [CrossRef Medline](#)
36. Fabiano AJ, Horsfield MA, Bakshi R. **Interhemispheric asymmetry of brain diffusivity in normal individuals: a diffusion-weighted MR imaging study.** *AJNR Am J Neuroradiol* 2005;26:1089–94 [Medline](#)
37. Bede P, Elamin M, Byrne S, et al. **Sexual dimorphism in ALS: exploring gender-specific neuroimaging signatures.** *Amyotroph Lateral Scler Frontotemporal Degener* 2014;15:235–43 [CrossRef Medline](#)
38. Chiu T, Fang D, Chen J, et al. **A robust and scalable clustering algorithm for mixed type attributes in large database environment.** In: *Proceedings of the seventh ACM SIGKDD international conference on knowledge discovery and data mining.* New York, New York, August 2001:263–68 [CrossRef](#)
39. Kaufman L, Rousseeuw PJ. **Finding groups in data: an introduction to cluster analysis.** *Biometrics* 1991;47:788 [CrossRef](#)
40. Spinelli EG, Riva N, Rancoita PMV, et al. **Structural MRI outcomes and predictors of disease progression in amyotrophic lateral sclerosis.** *Neuroimage Clin* 2020;27:102315 [CrossRef Medline](#)
41. Brettschneider J, Del Tredici K, Toledo JB, et al. **Stages of pTDP-43 pathology in amyotrophic lateral sclerosis.** *Ann Neurol* 2013;74:20–38 [CrossRef Medline](#)
42. Schito P, Spinelli EG, Malvaso A, et al. **Primary lateral sclerosis presenting with focal onset spreading through contiguous neuroanatomic regions.** *Neurology* 2022;98:503–04 [CrossRef Medline](#)
43. Ravits J. **Focal, stochastic and neuroanatomic propagation in ALS pathogenesis.** *Exp Neurol* 2014;262:121–26 [CrossRef Medline](#)
44. Sekiguchi T, Kanouchi T, Shibuya K, et al. **Spreading of amyotrophic lateral sclerosis lesions—multifocal hits and local propagation?** *J Neurol Neurosurg Psychiatry* 2014;85:85–91 [CrossRef Medline](#)
45. Ferraro PM, Cabona C, Meo G, et al. **Age at symptom onset influences cortical thinning distribution and survival in amyotrophic lateral sclerosis.** *Neuroradiology* 2021;63:1481–87 [CrossRef Medline](#)
46. Angenstein F, Niessen HG, Goldschmidt J, et al. **Age-dependent changes in MRI of motor brain stem nuclei in a mouse model of ALS.** *Neuroreport* 2004;15:2271–74 [CrossRef Medline](#)
47. Ferraro PM, Campi C, Miceli A, et al. **18F-FDG-PET correlates of aging and disease course in ALS as revealed by distinct PVC approaches.** *Eur J Radiol Open* 2022;9:100394 [CrossRef Medline](#)
48. Trojsi F, Di Nardo F, Caiazzo G, et al. **Between-sex variability of resting state functional brain networks in amyotrophic lateral sclerosis (ALS).** *J Neural Transm (Vienna)* 1996;2021;128:1881–97 [CrossRef Medline](#)
49. Chiò A, Moglia C, Canosa A, et al. **ALS phenotype is influenced by age, sex, and genetics: a population-based study.** *Neurology* 2020;94:e802–10 [CrossRef Medline](#)
50. Finegan E, Chipika RH, Li Hi Shing S, et al. **The clinical and radiological profile of primary lateral sclerosis: a population-based study.** *J Neurol* 2019;266:2718–33 [CrossRef Medline](#)
51. Tahedl M, Li H, Shing S, Finegan E, et al. **Propagation patterns in motor neuron diseases: Individual and phenotype-associated disease-burden trajectories across the UMN-LMN spectrum of MNDs.** *Neurobiol Aging* 2022;109:78–87 [CrossRef Medline](#)